

# Non-Lagrangian approach for coupled complex Ginzburg-Landau systems with higher order-dispersion

Roger Bertin Djob<sup>a,\*</sup>, Aurelien Kenfact-Jiotsa<sup>b</sup>, A. Govindarajan<sup>c</sup>

<sup>a</sup>Laboratory of Mechanics, Group of Nonlinear Physics and Complex Systems, Department of Physics, Faculty of Sciences, University of Yaounde I, P.O. Box 812, Yaounde, Cameroon

<sup>b</sup>Nonlinear Physics and Complex Systems Group, Department of Physics, Higher Teacher's Training College, University of Yaounde I, P.O. Box 47 Yaounde, Cameroon

<sup>c</sup>Centre for Nonlinear Dynamics, School of Physics, Bharathidasan University, Tiruchirappalli - 620 024, India

---

## Abstract

It is known that after a particular distance of evolution in fiber lasers, two (input) asymmetric soliton like pulses emerge as two (output) symmetric pulses having same and constant energy. We report such a compensation technique in dispersion managed fiber lasers by means of a semi-analytical method known as collective variable approach (CVA) with including third-order dispersion (TOD). The minimum length of fiber laser, at which the output symmetric pulses are obtained from the input asymmetric ones, is calculated for each and every pulse parameters numerically by employing Runge-Kutta fourth order method. The impacts of intercore linear coupling, asymmetric nature of initial parameters and TOD on the evolution of pulse parameters and on the minimum length are also investigated. It is found that strong intercore linear coupling and asymmetric nature of input pulse parameters result in the reduction of fiber laser length. Also, the role of TOD tends to increase the width of the pulses as well as their energies. Besides, chaotic patterns and bifurcation points on the minimum length of the fiber owing to the impact of TOD are also reported in a nutshell.

**Keywords:** Dual-core fiber lasers, Dispersion-management technique, Collective variable approach, Ginzburg-Landau equations, Third-order dispersion

---

## 1. INTRODUCTION

In nonlinear science, complex Ginzburg-Landau equations (CGLEs) serve as well-known models to represent ubiquitous nonlinear dynamics representing pattern formation and solitons for a number of media, which include reaction-diffusion systems, hydrodynamics, plasma systems, nonlinear optics and so forth [1–9]. In the context of nonlinear optics, the CGLE is obtained as a perturbation to the standard nonlinear Schrodinger equation (NLSE) for a system of fiber laser (of single and coupled versions) taking into account gain, loss and spectral filtering [10]. For a detailed review, readers can refer to [11, 12]. Among different types of fiber lasers, dual-core ring lasers have been receiving a widespread interest owing to their numerous applications in photonics [13–19]. Nonlinear directional couplers (NLDC) are one of important components of integrated optical devices and they deliver quite a few lightwave applications including switching (bright and dark) [20–27], logical operations [28, 29], ultra-short pulse generation through modulational instability [30–35], and amplifiers [36, 37]. In particular, Winful and Walton have proven that the asymmetric dual core fibers can act as a passive mode-locking fiber laser provided one of the dual-cores must be doped with rare earth-elements like erbium while the other core must be a passive one [3]. Such a device has successfully demonstrated a soliton generation with a huge amplification [38]. Following the former work, Kanka has numerically proposed a more realistic fiber laser employing Lorentzian resonant gain profile including stimulated Raman scattering [39]. A ring type fiber laser has been put forward by Oh *et al.* by considering higher order dispersion

---

\*Corresponding author

Email addresses: rogerdjob@yahoo.fr (Roger Bertin Djob), govind.nld@gmail.com (A. Govindarajan)

such as third-order dispersion and it has been reported that TOD and self-steepening do not alter the soliton generation substantially [40].

Along similar lines, quite a few theoretical studies have been emerged in the literature in order to identify the stability nature of such solitons. Especially, Malomed and Winful have reported the first ever stable solitons in the coupled fiber systems though the earlier observed one was completely unstable [13]. In addition, stable bound non-stationary solitons were also identified in the framework of coupled CGL systems [41]. Moreover, the instability conditions and nonlinear development of modulational instability were also reported [30, 42, 43]. These studies employing nonlinear waves, especially solitary waves, clearly exhibit that such fiber lasers based on coupled CGLEs can manifest a number of applications in lightwave communication systems [11]. Meanwhile, the study of dispersion management in optical fibers receives considerable interest. It is important to note that instead of using fibers with only anomalous dispersion as in case of soliton mode locking, dispersion managed solitons are generated by utilizing a dispersion map where normal and anomalous dispersions in fibers are periodically displaced [44].

The utilization of dispersion map is usually referred as dispersion management (DM) and the pertaining solutions are further referred as DM solitons. In this technique, the dispersion parameter is related to the GVD by the following relation; since the dispersion is a function of propagation distance, the pulse experiences periodic net balance between dispersion and nonlinearity at different positions and thus the pulse duration and chirp oscillate periodically along the propagation, which is why DM solitons are also called *stretched pulses*. On average, the pulse in the dispersion map broadens due to the net anomalous dispersion which should be exactly balanced by the nonlinearity and thus it goes back to its initial pulse width and spectrum bandwidth after each round-trip propagation [45]. Thus these breathing pulses can still be viewed as solitons on the average sense and are good candidate for mode locked fiber lasers since the periodic cavity boundary condition can be easily satisfied. Interestingly, these stretched pulses can also be generated from a cavity with small net normal dispersion. DM solitons have drawn significant attentions since the alternating sign of dispersions (normal and anomalous) helps suppressing the nonlinear phase accumulation which results in higher energies, usually by one order of magnitude, in comparison to the conventional soliton lasers. Besides, the breathing property of DM solitons helps to suppress the Gordon- Haus timing jitter in optical communication systems [46].

It is important to consider the higher order effects such as third-order dispersion (TOD), self-steepening and stimulated Raman scattering if the width of the pulse is considered to be 100 fs or even below [47–49]. In particular, the TOD parameter is more important in optical communications and one should consider when the pump wavelength is very close to zero group velocity dispersion. The importance of TOD term in models of fiber lasers has been well described in the literature. To enumerate them, Fewo *et al.* have investigated the role of TOD parameter in fiber amplifiers by means of collective variable analysis with the inclusion of quintic nonlinearity. They have also illustrated the influence of the third order dispersion and the cubic-quintic (CQ) nonlinear coefficients on the evolution of soliton pulses for different pulse parameters. Quite recently, Sakaguchi *et al.* have shown that the model of fiber-laser cavities near the zero dispersion point, based on the Complex Ginzburg-Landau equation with the cubic-quintic nonlinearity and TOD term, supports stable dissipative solitons and demonstrated that the same model gives rise to several specific families of robust bound states of solitons [50].

Recently, we have highlighted the interaction between two Gaussian pulses propagating in such a fiber laser by the means of collective variables approach [51]. This interaction was governed by a pair of CQ-CGLE without higher order dispersion (HOD) terms. The main result was the compensation of the energies between both cores whatever the input amplitudes and widths. Along these directions, one of the basic and necessary problems is to generate soliton sources with suitable physical and practical characteristics, such as compact and stable source of interest, compact size, and commercially available one [52]. Nevertheless, no study is focused on the dispersion management technique of dual-core fiber ring lasers based on the TOD effect and to determine the *minimum distance* after which the energies of input asymmetric pulses in neighbouring cores become constant and equal each other. Indeed, the issue of symmetric output pulses is relevant as the equal energy in the neighbouring cores of the fiber avoid compensation, no fluctuations and the energy of the emerging pulses can easily be evaluated. Motivated by all these facts, in this paper, we present a comprehensive picture of TOD term on the pulse shaping of optical solitons and identify the minimum length at which one obtains the symmetric bright solitons pair in the proposed system. To fulfil this goal, the paper is organized as follows. In Sec. 2, we derive the equations of motion from the CVs approach and briefly explain the dispersion management technique leading to the propagation of conventional solitons. In Sec. 3, we present a semi-analytical approach, which leads to determine the minimum distance or minimum length of the fiber

for obtaining symmetric output pulses. Finally, in Sec. 4 we conclude the paper.

## 2. Theoretical model and analytical techniques

The theoretical model of the present work is based on the linearly coupled CQ-CGLEs with the third order dispersion parameter, which can be written as

$$\begin{aligned} i\Psi_{1,x} + (p_r + ip_i)\Psi_{1,tt} + (q_r + iq_i)|\Psi_1|^2\Psi_1 &= i(\gamma_r + i\gamma_i)\Psi_1 + (c_r + ic_i)|\Psi_1|^4\Psi_1 + i(d_r + id_i)\Psi_{1,ttt} + k\Psi_2 \\ i\Psi_{2,x} + (p_r + ip_i)\Psi_{2,tt} + (q_r + iq_i)|\Psi_2|^2\Psi_2 &= i(\gamma_r + i\gamma_i)\Psi_2 + (c_r + ic_i)|\Psi_2|^4\Psi_2 + i(d_r + id_i)\Psi_{2,ttt} + k\Psi_1, \end{aligned} \quad (1)$$

where  $\Psi_i$  ( $i = 1, 2$ ) are normalized (in soliton units) complex envelopes of the field components (ie.,  $\Psi_1$  is the propagating field inside the core 1 and  $\Psi_2$  refers to the field inside the core 2) and  $t$  and  $x$  are, respectively, the normalized distance and the retarded time. Also, the parameters  $p_r$ ,  $p_i$ ,  $d_r$ ,  $d_i$ ,  $q_r$ ,  $q_i$ ,  $c_r$ ,  $c_i$ ,  $\gamma_r$  and  $\gamma_i$  are real constants and in what follows, without loss of generality, they can be commonly expressed as a function of  $x$  without loosing their constant characters, viz.,  $p_r = p_r(x)$ ,  $p_i = p_i(x)$ ,  $d_r = d_r(x)$ ,  $d_i = d_i(x)$ ,  $q_r = q_r(x)$ ,  $q_i = q_i(x)$ ,  $c_r = c_r(x)$ ,  $c_i = c_i(x)$ ,  $\gamma_r = \gamma_r(x)$ , and  $\gamma_i = \gamma_i(x)$ , respectively. Further, it is to be noted that the term  $p_r$  measures the wave dispersion while  $p_i$  denotes the spectral filtering coefficient. Likewise,  $d_r$  is the TOD coefficient,  $d_i$  the cubic frequency dependent gain/loss coefficient,  $q_r$  and  $q_i$  accordingly represent the nonlinear coefficient and nonlinear gain-absorption parameters. It is worthwhile to mention that the nonlinear gain helps to suppress the growth of radiative background (linear mode) which always accompanies the propagation of nonlinear stationary pulses in real fiber links. Furthermore,  $c_r$  and  $c_i$  stand for the higher-order correction terms to the nonlinear refractive index and nonlinear amplification absorption, respectively. The other terms  $\gamma_r$  and  $\gamma_i$  represent the linear gain and frequency shift, respectively whereas the inter core linear coupling coefficient is noted through the parameter  $k$ .

### 2.1. Collective variables approach

In the context of nonlinear fiber optics, there exist a few analytical methods to study the dynamics of optical pulses. If we consider the effects of optical losses, and higher order dispersion including non-paraxial limit, the non-integrable nature tend to make them hard to study analytically and one has to seek the aid of relevant numerical methods [53]. Nevertheless, a non-Lagrangian method, namely collective variable approach (CVA) can be employed to any perturbative NLSE as it does not require any conserved energy to reduce the governing equations [54–56]. Hence, it is possible to derive the CV equations for the perturbative NLSE which makes them very useful to study the former. It is well-known that the collective variable approach is mainly dependent on the separation of original applied fields  $\Psi_j$ , ( $j = 1, 2$ ) into some appropriate functions known as ansatzes ( $f_1$  and  $f_2$ ) with residual fields ( $g_1$  and  $g_2$ ) as

$$\begin{aligned} \Psi_1(x, t) &= f_1(u_1, \dots, u_N, t) + g_1(x, t) \\ \Psi_2(x, t) &= f_2(v_1, \dots, v_N, t) + g_2(x, t), \end{aligned} \quad (2)$$

where  $u_i$  and  $v_i$  are space-dependent variables and can describe the nature of applied fields. Let us now consider the Gaussian ansatzes, which read as

$$\begin{aligned} f_1(u_1, u_2, u_3, u_4, u_5, u_6, t) &= u_1 e^{-\frac{(t-u_2)^2}{u_3^2}} e^{i\frac{u_4}{2}(t-u_2)^2 + iu_5(t-u_2) + iu_6} \\ f_2(v_1, v_2, v_3, v_4, v_5, v_6, t) &= v_1 e^{-\frac{(t-v_2)^2}{v_3^2}} e^{i\frac{v_4}{2}(t-v_2)^2 + iv_5(t-v_2) + iv_6}. \end{aligned} \quad (3)$$

In Eq. (3), the collective variables  $u_1$ ,  $u_2$ ,  $\sqrt{2\ln(2)}u_3$ ,  $\frac{u_4}{2\pi}$ ,  $\frac{u_5}{2\pi}$  and  $u_6$  accordingly indicate the pulse amplitude, temporal position, pulse width (FWHM), chirp, frequency and phase of the pulse propagating in the first core, while other terms such as  $v_1$ ,  $v_2$ ,  $\sqrt{2\ln(2)}v_3$ ,  $\frac{v_4}{2\pi}$ ,  $\frac{v_5}{2\pi}$  and  $v_6$  refer the same as defined in the above for the second core of the fiber laser.

To determine the role each collective variables, one has to reduce the number of terms in the residual field energies. The expressions of the residual field energies are written

$$\begin{aligned}\varepsilon_1 &= \int_{-\infty}^{+\infty} |g_1(x, t)|^2 dt = \int_{-\infty}^{+\infty} |\Psi_1(x, t) - f_1(u_i, t)|^2 dt \\ \varepsilon_2 &= \int_{-\infty}^{+\infty} |g_2(x, t)|^2 dt = \int_{-\infty}^{+\infty} |\Psi_2(x, t) - f_2(v_i, t)|^2 dt, i = 1..N;\end{aligned}\quad (4)$$

Also, the total energy calculated in each of cores can be further read as

$$\begin{aligned}E_1 &= \int_{-\infty}^{+\infty} |\Psi_1(x, t)|^2 dt \\ E_2 &= \int_{-\infty}^{+\infty} |\Psi_2(x, t)|^2 dt.\end{aligned}\quad (5)$$

Hence, the expressions for the calculated energy of the residual fields become

$$\begin{aligned}\varepsilon_1 &= \int_{-\infty}^{+\infty} |f_1(u_i, t)|^2 dt - 2R_e\left(\int_{-\infty}^{+\infty} \Psi_1(x, t)f_1^*(u_i, t) dt\right) \\ \varepsilon_2 &= \int_{-\infty}^{+\infty} |f_2(v_i, t)|^2 dt - 2R_e\left(\int_{-\infty}^{+\infty} \Psi_2(x, t)f_2^*(v_i, t) dt\right),\end{aligned}\quad (6)$$

Note that \* indicates the complex conjugate.

If one knows the ansatzes that must satisfy the minimization of the residual field energies, we can then obtain the first constraint equations of the form

$$\begin{aligned}C_i^1 &= \frac{\partial \varepsilon_1}{\partial u_i} \\ C_i^2 &= \frac{\partial \varepsilon_2}{\partial v_i}.\end{aligned}\quad (7)$$

which can also be read as

$$\begin{aligned}C_i^1 &= 2R_e\left(-\int_{-\infty}^{+\infty} g_1 f_{1,u_i}^* dt\right) \\ C_i^2 &= 2R_e\left(-\int_{-\infty}^{+\infty} g_2 f_{2,v_i}^* dt\right),\end{aligned}\quad (8)$$

where  $f_{1,u_i}$  and  $f_{2,v_i}$  indicate, respectively, the first derivatives of  $f_1$  and  $f_2$  with respect to pulse parameters  $u_i$  and  $v_i$ . Similarly, the second constraint equations of motions read as

$$\begin{aligned}\dot{C}_i^1 &= 0 \\ \dot{C}_i^2 &= 0;\end{aligned}\quad (9)$$

where the terms  $\dot{C}_i^1$  and  $\dot{C}_i^2$  are, respectively, the first derivatives with respect to  $x$  of  $C_i^1$  and  $C_i^2$ . Proceeding further, the second constraint equations are written as

$$\begin{aligned}\dot{C}_i^1 &= 2R_e\left[-\int_{-\infty}^{+\infty} g_1 f_{1,u_i u_j}^* dt - \int_{-\infty}^{+\infty} g_{1,x} f_{1,u_i}^* dt\right] = 0 \\ \dot{C}_i^2 &= 2R_e\left[-\int_{-\infty}^{+\infty} g_2 f_{2,v_i v_j}^* dt - \int_{-\infty}^{+\infty} g_{2,x} f_{2,v_i}^* dt\right] = 0;\end{aligned}\quad (10)$$

Here, the term  $f_{x_i}$  is the first derivative with respect to  $x_i$  of  $f$ . Employing the *bare approximation* i.e.,  $g \approx 0$  and considering the slow variations of the residual fields with the time viz.,  $g_{tt} \approx 0$ , the constraint equations become further

$$\begin{aligned} \dot{C}_i^1 &= 2R_e \left[ \sum \left( \langle f_{1,u_i}^* \cdot f_{1,u_j} \rangle - \langle f_{1,u_i}^* \cdot i(p_r + ip_i) \cdot f_{1,tt} \rangle + \langle f_{1,u_i}^* \cdot (d_r + id_i) \cdot f_{1,ttt} \rangle \right. \right. \\ &\quad \left. \left. - \langle f_{1,u_i}^* \cdot (\gamma_r + i\gamma_i) \cdot f_1 \rangle - \langle f_{1,u_i}^* \cdot i(q_r + iq_i) \cdot |f_1|^2 f_1 \rangle \right. \right. \\ &\quad \left. \left. + \langle f_{1,u_i}^* \cdot i(c_r + ic_i) \cdot |f_1|^4 f_1 \rangle + \langle f_{1,v_i}^* \cdot k \cdot f_2 \rangle \right] = 0 \\ \dot{C}_i^2 &= 2R_e \left[ \sum \left( \langle f_{2,v_i}^* \cdot f_{2,v_j} \rangle - \langle f_{2,v_i}^* \cdot i(p_r + ip_i) \cdot f_{2,tt} \rangle + \langle f_{2,v_i}^* \cdot (d_r + id_i) \cdot f_{2,ttt} \rangle \right. \right. \\ &\quad \left. \left. - \langle f_{2,v_i}^* \cdot (\gamma_r + i\gamma_i) \cdot f_2 \rangle - \langle f_{2,v_i}^* \cdot i(q_r + iq_i) \cdot |f_2|^2 f_2 \rangle \right. \right. \\ &\quad \left. \left. + \langle f_{v_i}^* \cdot i(c_r + ic_i) \cdot |f_2|^4 f_2 \rangle + \langle f_{2,v_i}^* \cdot k \cdot f_1 \rangle \right] = 0, \end{aligned} \quad (11)$$

In all the above equations, the terms indicated in the closed parenthesis indicate the integration with respect to the time as,  $\langle \dots \rangle = \int_{-\infty}^{+\infty} (\dots) dt$  and  $R_e(\dots)$  refers to the real part of the complex  $(\dots)$ . The final constraint equations of motion for the pulse parameters can be read as

$$\begin{aligned} [\dot{C}^1] &= \left[ \frac{\partial C^1}{\partial U} \right] [\dot{U}] + [R^1] = 0 \\ [\dot{C}^2] &= \left[ \frac{\partial C^2}{\partial V} \right] [\dot{V}] + [R^2] = 0, \end{aligned} \quad (12)$$

which lead to,

$$\begin{aligned} [\dot{U}] &= - \left[ \frac{\partial C^1}{\partial U} \right]^{-1} [R^1] \\ [\dot{V}] &= - \left[ \frac{\partial C^2}{\partial V} \right]^{-1} [R^2], \end{aligned} \quad (13)$$

where  $\left[ \frac{\partial C^1}{\partial U} \right]$  and  $\left[ \frac{\partial C^2}{\partial V} \right]$  are square matrices whose elements are noted

$$\begin{aligned} C_{ij}^1 &= -2R_e \langle f_{1,u_i}^* \cdot f_{u_j} \rangle \\ C_{ij}^2 &= -2R_e \langle f_{2,v_i}^* \cdot f_{v_j} \rangle. \end{aligned} \quad (14)$$

While  $\left[ \frac{\partial C^1}{\partial U} \right]^{-1}$  and  $\left[ \frac{\partial C^2}{\partial V} \right]^{-1}$  are inverse matrices of  $\left[ \frac{\partial C^1}{\partial U} \right]$  and  $\left[ \frac{\partial C^2}{\partial V} \right]$ ,  $[R_i^{1,2}]$  are column vectors whose elements are written as

$$\begin{aligned} R_i^1 &= 2R_e \left( - \langle f_{1,u_i}^* \cdot i(p_r + ip_i) \cdot f_{1,tt} \rangle + \langle f_{1,u_i}^* \cdot (d_r + id_i) \cdot f_{1,ttt} \rangle - \langle f_{1,u_i}^* \cdot (\gamma_r + i\gamma_i) \cdot f_1 \rangle \right. \\ &\quad \left. - \langle f_{1,u_i}^* \cdot i(q_r + iq_i) \cdot |f_1|^2 f_1 \rangle + \langle f_{1,u_i}^* \cdot i(c_r + ic_i) \cdot |f_1|^4 f_1 \rangle + \langle f_{1,u_i}^* \cdot k \cdot f_2 \rangle \right) \\ R_i^2 &= 2R_e \left( - \langle f_{2,v_i}^* \cdot i(p_r + ip_i) \cdot f_{2,tt} \rangle + \langle f_{2,v_i}^* \cdot (d_r + id_i) \cdot f_{2,ttt} \rangle - \langle f_{2,v_i}^* \cdot (\gamma_r + i\gamma_i) \cdot f_2 \rangle \right. \\ &\quad \left. - \langle f_{2,v_i}^* \cdot i(q_r + iq_i) \cdot |f_2|^2 f_2 \rangle + \langle f_{2,v_i}^* \cdot i(c_r + ic_i) \cdot |f_2|^4 f_2 \rangle + \langle f_{2,v_i}^* \cdot k \cdot f_1 \rangle \right). \end{aligned} \quad (15)$$

Applying all the above developments, one obtains the equations of motion of the pulse parameters as given in Appendix A

## 2.2. The dispersion management technique

The dispersion management technique aims to form non-conventional soliton by alternating normal ( $p_r < 0$ ) and anomalous ( $p_r > 0$ ) dispersions and assuring overall zero dispersion. Its principle consists of anomalous-dispersion ( $p_r = d_1 > 0$ ) section with a length  $z_1$ , followed by a normal-dispersion ( $p_r = d_2 < 0$ ) section with a length  $z_2$  respecting the zero-average dispersion as written in the following form

$$d_1 z_1 + d_2 z_2 \approx 0 \quad (16)$$

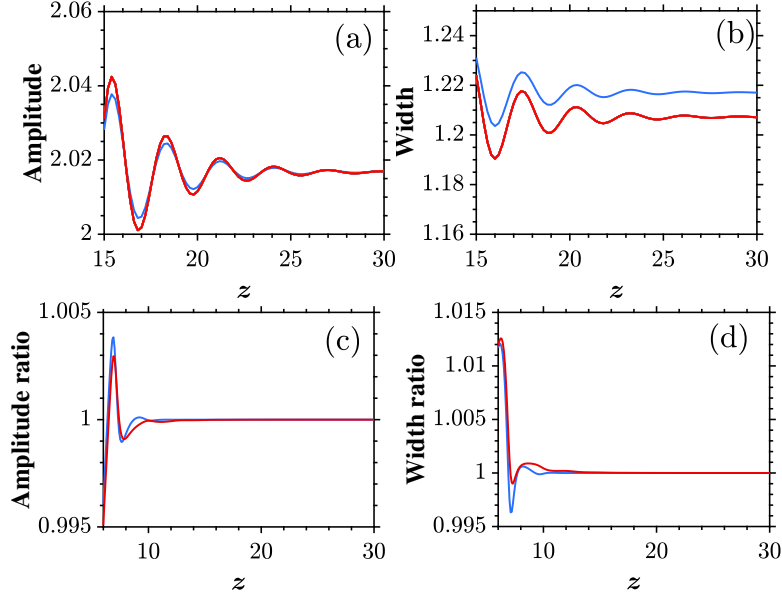


Figure 1: *Effect of TOD on the spatial evolution of amplitudes and widths of input asymmetric gaussian pulses in the first core of fiber laser (the dynamics in the second core is not shown as it exhibits almost the same dynamics as in the first core). The blue curves correspond to  $d_r = 0.0$  and the red curves are drawn with  $d_r = -0.1$ . The initial parameters values are chosen such that  $u_{10} = u_{30} = 1$ ,  $v_{10} = 0.75$ ,  $v_{30} = 1$  and the coupling coefficient value is to be,  $k = 0.5$ .*

It must be noted that in this work, we fix the length of fiber laser as  $z_1 = 0.025$ ,  $z_2 = 0.025$  (corresponding to the anomalous and normal dispersion regimes) and the group velocity dispersion coefficient to be  $p_r = 0.5$  and  $p_r = -0.5$  for the anomalous and normal dispersion regimes, respectively. The numerical study pertaining to the evolution of neighboring pulse parameters along the propagation distance is carried out using the standard Runge–Kutta fourth order method with a spatial step size of  $2 \times 10^{-3}$ .

### 3. Results and discussions

#### 3.1. Spatial evolution of input asymmetric pulses

To launch the input pulses, we consider the asymmetric soliton like pulses (gaussian) that attain the asymmetric nature either in their amplitude or widths ( $u_i \neq v_i$ ) expect the condition imposed on the temporal position as  $u_2 = -v_2$ . Note that the other parameters will remain same in both cores as ( $u_{40} = v_{40} = 1$ ,  $u_{50} = v_{50} = 1$ ,  $u_{60} = v_{60} = 1$  and  $u_2 = -v_2 = 1$ ). As we have considered our model to be CQ-CGLEs which are obtained as a perturbation to the standard NLSE, we assign the parameters  $p_i$ ,  $q_i$ ,  $c_i$  to be very small, viz.,  $p = 1 - i0.6$ ,  $q = 1 - i0.046$ ,  $c = 0.1 + i0.0016$ ,  $d_i = 0.01$ ,  $\gamma_r = 0.001$  and  $\gamma_i = 0$ . Also, as mentioned in the description of non-Lagrangian method, throughout the analysis numerical computations will be done for the zero-average dispersion in the fiber lasers.

We first study the role of TOD on the pulse evolution inside the fiber cores as depicted in Fig. 1. As seen from the figure, it is clear to observe that the width and amplitude in each core fluctuate at the beginning of the longitudinal distance prior to the stabilization (see Figs. 1(a) and 1(b)). Once they settle themselves by stabilizing, the pulses in both cores feature constant value with respect to another neighboring core. The bottom panels in Fig. 1 reveals the dynamics of amplitude and width ratios and it can be inferred that the amplitude ratio and width ratio of waves propagating in the two cores primarily oscillate before stabilizing to unity in their values after a certain distance. One can further observe that we have also focused on the roles of different input settings in the fiber lasers as shown in Fig. 2. From this figure, it comes that when the initial asymmetry concerns only the amplitudes 2(a-b), the amplitude and width ratios stabilize faster (the distance of fluctuations is shorter) to unity and the peaks of fluctuations are lower. However, when the initial asymmetry concerns the widths 2(c-d), the distance of fluctuations is larger. For total

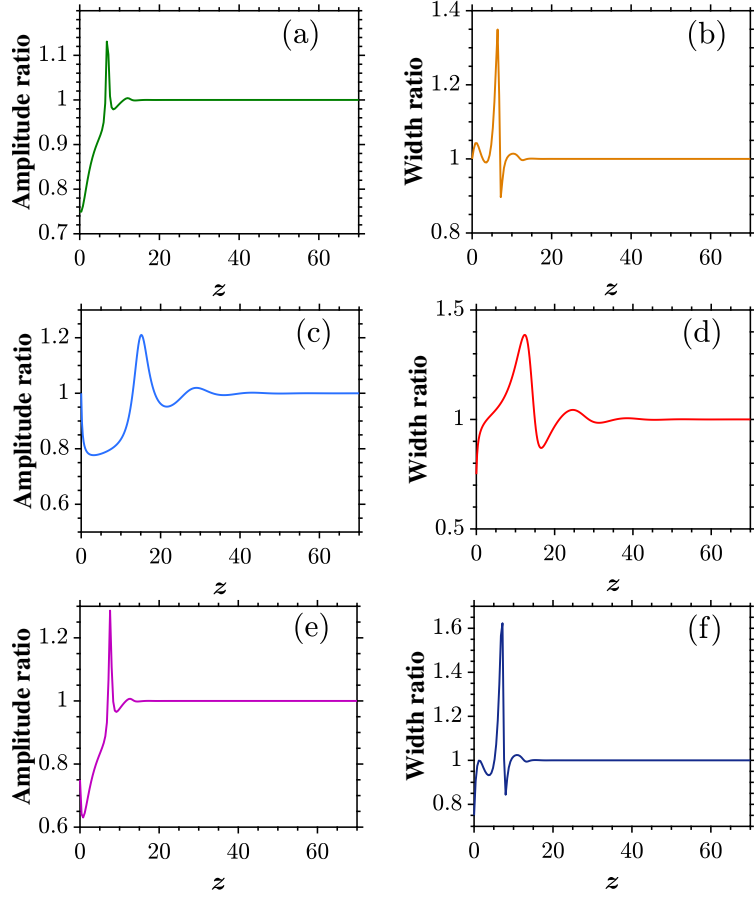


Figure 2: *Spatial evolution of amplitude ratio and width ratio of input asymmetric gaussian pulses in the two cores. (a-b):  $u_{10} = u_{30} = 1$ ,  $v_{10} = 0.75$ ,  $v_{30} = 1$ ; (c-d):  $u_{10} = u_{30} = 1$ ,  $v_{10} = 1$ ,  $v_{30} = 0.75$ ; and (e-f):  $u_{10} = u_{30} = 1$ ,  $v_{10} = 0.75$ ,  $v_{30} = 0.75$ . The other system parameters are  $k = 0.01$ , and  $d_r = -0.008$ .*

asymmetry i.e asymmetry on initial amplitude and widths 2(e-f), the peaks of fluctuations of amplitudes and widths is higher but the distance of fluctuations is shorter than in the second case. One can then conclude that the initial asymmetry on amplitudes is more suitable for shorter minimum length (i.e distance at which amplitudes and widths are superposed).

In addition to the above ramifications, we have also studied the evolution of energies of waves propagating inside each core. Their expressions are respectively given in the following relations

$$E_1 = \int_{-\infty}^{\infty} (|f_1|)^2 dt = \sqrt{\frac{\pi}{2}} u_1^2 u_3, \text{ and} \quad (17)$$

$$E_2 = \int_{-\infty}^{\infty} (|f_2|)^2 dt = \sqrt{\frac{\pi}{2}} v_1^2 v_3. \quad (18)$$

Observations of Figs. 1 and 2 are confirmed in Fig. 3 which shows the variations of wave energies in each core. One can observe from these figures that the cores exchange their energies at the beginning of the propagation, the one with the higher energy transfers it to the other core before reaching an equilibrium state where the energies are superposed (equal). Also, Fig. 3 reveals that, the energies become equal once the parameters (amplitudes and widths) get the same value. Indeed in this case, both amplitude and width ratios are equal to one. Besides, Fig. 4 presents the effect of the TOD on the energy in the first core at the equilibrium state. One can now observe that in the presence of TOD ( $d_r = -0.1$ ), the constant energy at the equilibrium state is higher (red curve). In the following, we study the



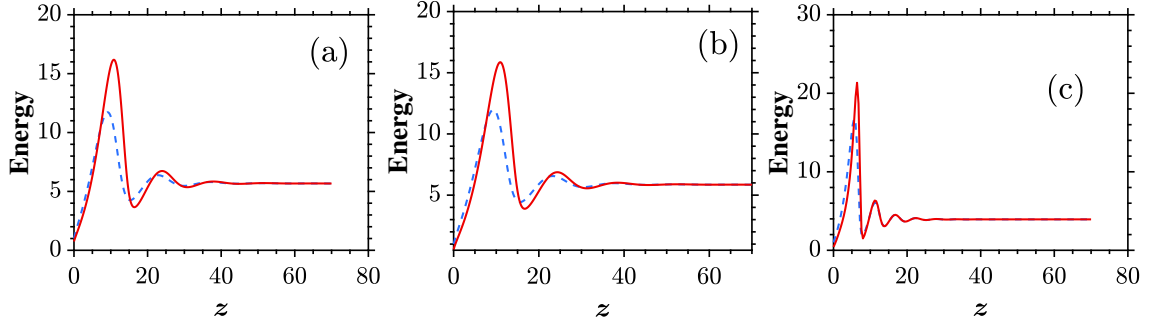


Figure 3: Spatial evolution of energies of input asymmetric gaussian pulses in the two cores of the fiber laser. The blue curves correspond to the evolution in core 1 and the red curves are meant for the evolution in core 2. The system parameters are (a):  $u_{10} = u_{30} = 1$ ,  $v_{10} = 0.75$ ,  $v_{30} = 1$ ; (b):  $u_{10} = u_{30} = 1$ ,  $v_{10} = 1$ ,  $v_{30} = 0.75$ ; and (c):  $u_{10} = u_{30} = 1$ ,  $v_{10} = 0.75$ ,  $v_{30} = 0.75$ . In all plots, the other parameters are chosen such that  $k = 0.01$  and  $d_r = -0.008$

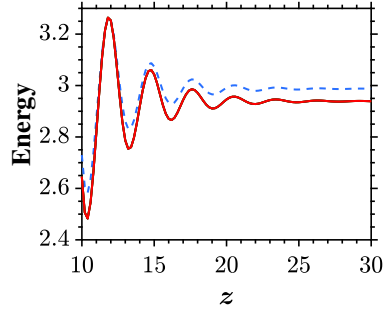


Figure 4: Impact of TOD on the spatial evolution of energies of input asymmetric gaussian pulses in the fiber laser. The blue curve corresponds to  $d_r = 0.0$  and the red curve denotes  $d_r = -0.1$ . The initial parameters values are  $u_{10} = u_{30} = 1$ ,  $v_{10} = 0.75$ ,  $v_{30} = 1$ , and  $k = 0.5$ .

influence of the coupling coefficient, initial parameters and the TOD on the minimum distance after which the energy diagrams in each core are superposed and determine numerically the values of these distances in each case.

### 3.2. Determining the minimum length of the fiber laser

Following Eqs. 17 and 18, the energy ratio reads as

$$E_{ratio} = \frac{E_2}{E_1} = \frac{v_1^2 v_3}{u_1^2 u_3}. \quad (19)$$

In order to obtain output symmetric pulses, the minimum length of the fiber laser is obtained numerically. This operation is performed to determine the energy ratio closer to 1 ( $E_{ratio} = 1$ ) meaning that either the parameters are equal in both cores i.e  $u_1 = v_1$  and  $u_3 = v_3$  or the energies of pulses in the neighbouring cores are equal. Thus, we fix a condition in the Runge-Kutta program as,

$$|E_{ratio} - 1| < \epsilon; \quad (20)$$

where  $\epsilon$  is an extremely small value, which takes  $\epsilon = 10^{-6}$ .

#### 3.2.1. Influence of inter-core coupling on the minimum length of the fiber

Figure 5 is plotted to investigate the spatial evolution of energy ratio i.e the ratio between the energy of the pulse in core 2 over the energy of the pulse in core 1 by adopting Eq. 19 for different values of the coupling coefficient. As seen in the figure, one can clearly notice that the energy ratio stabilizes to 1 and more faster on increasing the coupling constant. These values can be noted as follows, for  $k = 0.01$ ,  $L_{min} = 57.410$  (Fig. 5(a)), for  $k = 0.1$ ,



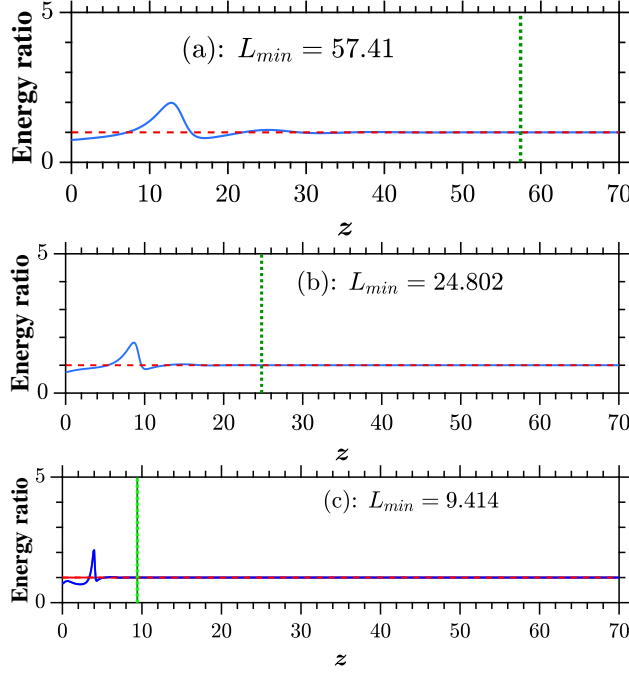


Figure 5: Evolution of energy ratio for different values of the coupling coefficient. (a):  $k = 0.01$ , (b):  $k = 0.1$  and (c):  $k = 0.5$ . The initial parameters values are  $u_{10} = u_{30} = 1$ ,  $v_{10} = 0.75$ ,  $v_{30} = 1$ , and  $d_r = -0.008$

$L_{min} = 28.802$  (Fig. 5(b)) and for  $k = 0.5$ ,  $L_{min} = 9.414$  (Fig. 5(c)). It is to be noted that the simulations are made for input asymmetric parameters as follows;  $u_{10} = 1$ ,  $v_{10} = 0.75$  and  $u_{30} = v_{30} = 1$ . Let us remember the dimensionless transformation [51];  $x = \frac{X}{L_D}$ , and  $L_D = \frac{T_0^2}{|\beta_2|}$ ;  $X$  being the real distance,  $L_D$  the dispersion length,  $T_0$  the width of the pulse and  $\beta_2$  the GVD coefficient (related to  $p_r$  through the relation  $p_r = \frac{\beta_2}{2}$ ). We adopt the physical parameters corresponding to standard nonlinear directional couplers, as follows [22]:  $\beta_2 = 0.02ps^2/m$ ,  $T_0 = 50fs$  at  $\lambda = 1.5\mu m$ . From the latter, we estimate the minimum length of the fiber respectively as follows, 28.705, 14.401 and 4.707 in meters.

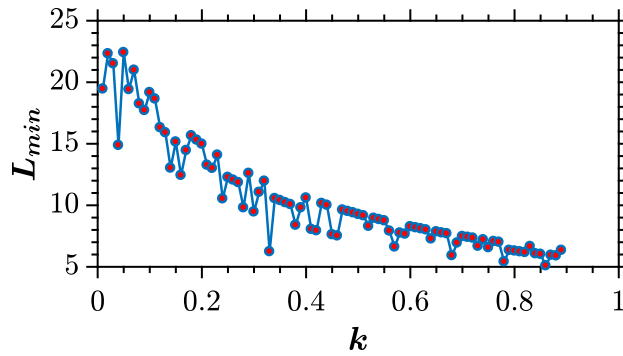


Figure 6: Evolution of the minimum length versus the coupling coefficient. The system parameters are chosen such that  $u_{10} = u_{30} = 1$ ,  $v_{10} = 0.75$ ,  $v_{30} = 1$  and  $d_r = -0.008$

The previous observations pertaining to the influence of the coupling constant on the minimum length are confirmed by Fig. 6 where  $L_{min}$  is plotted versus  $k$ , the coupling constant. This figure shows that  $L_{min}$  decreases quasi exponentially on increasing the value of  $k$ , even if there are some fluctuations. For the strong coupling i.e.  $k \rightarrow 1$ , the minimum length is quasi null ( $L_{min} \rightarrow 0$ ).

### 3.2.2. Influence of input amplitudes and widths on the minimum length of the fiber laser

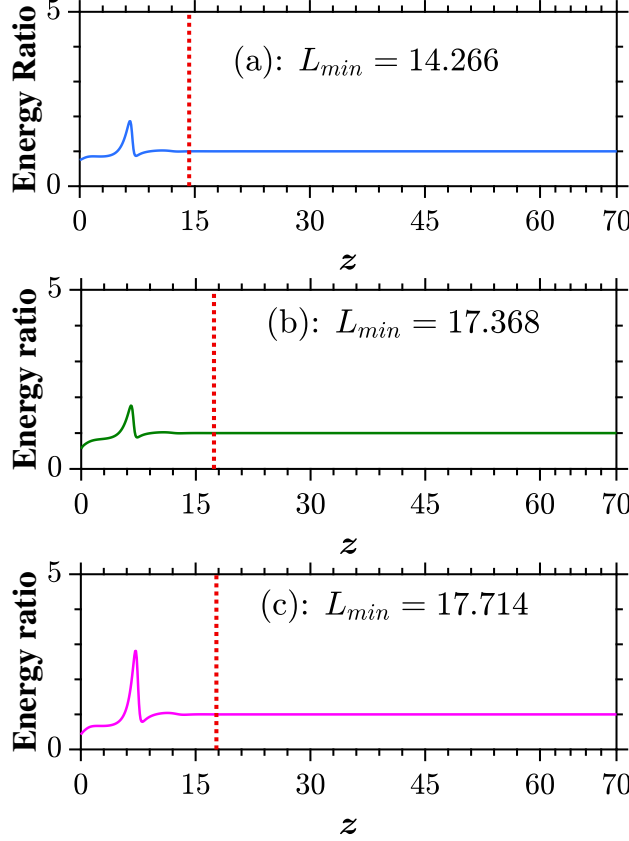


Figure 7: Evolution of energy ratio for different values of input parameters. (a):  $u_{10} = 1, v_{10} = 0.75, u_{30} = v_{30} = 1$ ; (b):  $u_{10} = v_{10} = 1, u_{30} = 1, v_{30} = 0.75$ ; and (c):  $u_{10} = 1, v_{10} = 0.75, u_{30} = 1, v_{30} = 0.75$ . The other system parameters are  $k = 0.01$ , and  $d_r = -0.008$

Figure 7 illustrates the spatial evolution of energy ratio for different values of the input amplitudes and widths. One can find from the figure that the minimum length is larger (as observed in Fig. 7 (c)) corresponding to full initial asymmetry viz., different input amplitudes and different input widths. Indeed, we achieve the following minimum length as,  $L_{min} = 14.266$  when  $u_{10} = 1, v_{10} = 0.75, u_{30} = v_{30} = 1$  (Fig. 7(a));  $L_{min} = 17.368$  when  $u_{10} = v_{10} = 1, u_{30} = 1, v_{30} = 0.75$  (Fig. 7(b)) and  $L_{min} = 17.714$  when  $u_{10} = 1, v_{10} = 0.75, u_{30} = 1, v_{30} = 0.75$  (Fig. 7(c)). From these ramifications, we estimate the minimum length of the fiber laser respectively to: 7.133, 8.684 and 8.857 in meters. Another observation from the figure is that the maximum ratio is higher on Fig. 7(c) compared to those of Fig. 7(a) and Fig. 7(b). This is obvious since there is more compensation when there are many input different parameters.

### 3.2.3. Influence of the third order dispersion on the minimum length of the fiber

Figure 8 depicting the spatial evolution of energy ratio for different values of the third order dispersion coefficient reveals that this TOD coefficient acts in a strange manner. While increasing  $d_r$ , one was expecting the minimum length to change in one way i.e may be increasing or decreasing. Nevertheless, one observes that for  $d_r = -0.008$ ,  $L_{min}$  is evaluated to 54.070; for  $d_r = -0.01$ ,  $L_{min}$  is evaluated to 61.772; while for  $d_r = -0.05$ ,  $L_{min}$  is evaluated to 53.870. Corresponding real values are, respectively, 27.035, 30.886 and 26.935 in meters. To explain these observations, we have also plotted the evolution of the minimum length versus the third order dispersion coefficient in Fig. 9. This figure reveals a chaotic evolution of the minimum length beyond two bifurcation points. Indeed, while varying the TOD coefficient between  $d_r = -0.025$  and  $d_r = 0.06$ , we note that the minimum length is quasi-constant (just few fluctuations) and relatively lower. Before  $d_r = -0.025$  and after  $d_r = 0.06$ , the values of the minimum lengths

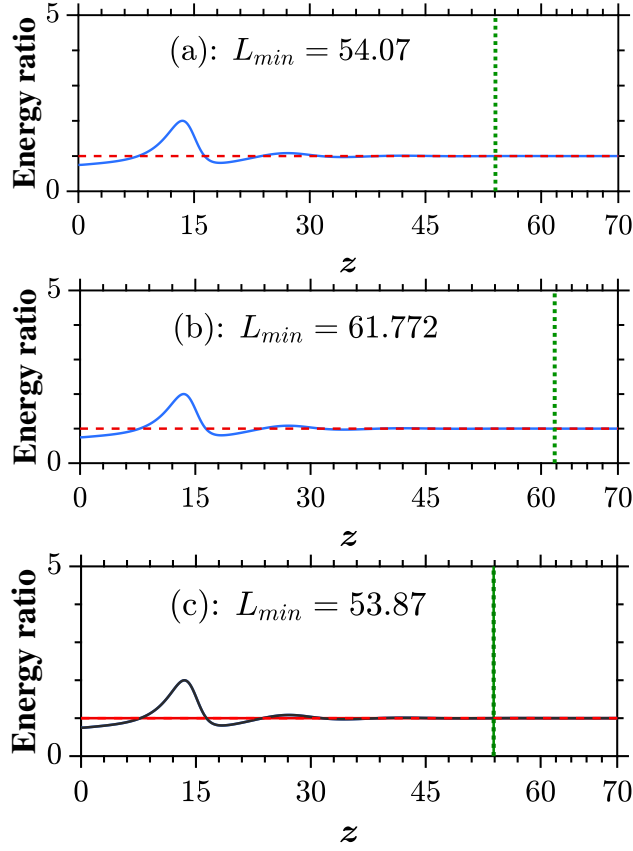


Figure 8: Plots depicting evolution of energy ratio for different values of third order dispersion (TOD) coefficient. (a):  $d_r = -0.008$ ; (b):  $d_r = -0.01$ ; and (c):  $d_r = -0.05$ . The initial parameters values are  $u_{10} = u_{30} = 1$ ,  $v_{10} = 0.75$ ,  $v_{30} = 1$ , and  $k = 0.01$ .

are unpredictable as the variations are in a random manner.

#### 4. Conclusions

We have done a systematic analysis pertaining to the dynamics of gaussian pulses in a system of fiber lasers by considering the third order parameter. From the results of the equations of motion of CVs parameters, we have determined numerically the minimum distance of propagation after which the pulses in two neighboring cores of a dual-core fiber laser can remain in constant and equal energy. This distance corresponds to the minimum length of the fiber for which asymmetric input pulses should result in symmetric output pulses. We have successfully obtained these values numerically by the means of the Runge Kutta algorithm following a non-Lagrangian approach. The analysis of the results show that the minimum length of the fiber is strongly influenced by the coupling, the initial asymmetry and the TOD. We have also found that strong coupling and total initial asymmetry favors the shorter minimum length of the fiber and we hope that these outcomes are beneficial for safe propagation of the neighboring pulses in a nonlinear dual-core fiber lasers. A remarkable aspect is noted when stressing the impact of TOD influence, namely, this parameter increases the common width and energy at the equilibrium state. We have also discovered a chaotic pattern beyond some bifurcation values while varying the TOD coefficient.

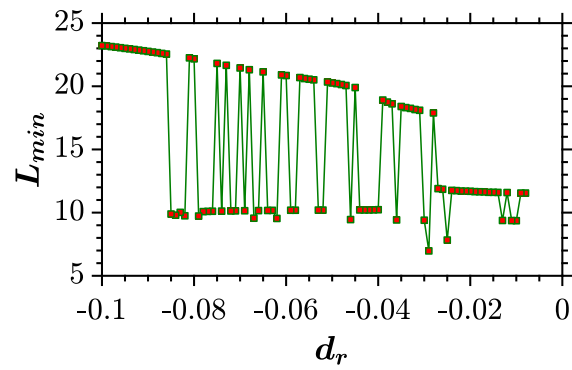


Figure 9: Evolution of the minimum length versus the third order dispersion (TOD) coefficient. The system parameters values are assigned  $u_{10} = u_{30} = 1, v_{10} = 0.75, v_{30} = 1,$  and  $k = 0.5$ .

## Appendix A. Equations of motions

$$\begin{aligned}
\dot{u}_1 &= -\frac{3}{2} \left[ \frac{\sqrt{2}}{(u_3^2 + v_3^2)^{\frac{5}{2}} u_3^2} \left[ \frac{4}{3} v_1 \left( -\frac{3}{4} u_3^4 + ((u_2^2 - v_2)^2 - v_3^2) u_3^2 - \frac{1}{4} v_3^4 \right) k u_3^2 v_3 e^{-\frac{(u_2 - v_2)^2}{u_3^2 + v_3^2}} \right. \right. \\
&\quad + \left. \left( \left( -\frac{1}{3} d_i u_5^3 + d_r u_4 u_5 - \frac{1}{3} u_5^2 p_i + \frac{1}{3} u_4 p_r - \frac{\gamma_r}{3} \right) u_3^2 - 2 d_i u_5 - \frac{2}{3} p_i \right) \sqrt{2} \right. \\
&\quad \left. \left. + \frac{4 u_1^2 u_3^2}{27} \left( u_1^2 \sqrt{6} c_i + \frac{45 q_i}{16} \right) \right] u_1 (u_3^2 + v_3^2)^{\frac{5}{2}} \right] \\
\dot{u}_2 &= \frac{3}{16} \left[ \frac{\sqrt{2}}{(u_3^2 + v_3^2)^{\frac{3}{2}} u_3^2 u_1} \left( -\frac{32 k v_1 v_3 u_3^4 (u_2 - v_2)}{3} e^{-\frac{(u_2 - v_2)^2}{u_3^2 + v_3^2}} + (d_i u_3^6 u_4^3 + 2 u_4 (2 d_i u_5^2 \right. \right. \\
&\quad \left. \left. + d_r u_4 + \frac{4}{3} p_i u_5) u_3^4 + (4 d_i u_4 + 8 u_5 (u_5 d_r + \frac{2}{3} p_r)) u_3^2 + 8 d_r u_1 \sqrt{2} (u_3^2 + v_3^2)^{3/2} \right) \right] \\
\dot{u}_3 &= \frac{3}{4} \frac{\sqrt{2}}{(u_3^2 + v_3^2)^{\frac{5}{2}} 16} u_3 u_1 \left[ \frac{16}{3} v_1 \left( -\frac{1}{4} u_3^4 + u_3^2 (u_2 - v_2)^2 + \frac{1}{4} v_3^4 \right) k u_3^2 v_3 e^{-\frac{(u_2 - v_2)^2}{u_3^2 + v_3^2}} + \left( (u_4^2 (d_i u_5 + \frac{p_i}{3}) u_3^4 \right. \right. \\
&\quad \left. \left. + 4 u_4 (u_5 d_r + \frac{p_r}{3}) u_3^2 - 4 d u_5 - \frac{4}{3} p_i \right) \sqrt{2} + \frac{4 u_1^2 (u_1^2 \sqrt{6} c_i + \frac{9}{4} q_i) u_3^2}{27} \right] u_1 (u_3^2 + v_3^2)^{\frac{5}{2}} \\
\dot{u}_4 &= -3 \left[ \frac{\sqrt{2}}{(u_3^2 + v_3^2)^{\frac{5}{2}} u_3^4 u_1} \left( -\frac{16}{3} v_1 \left( \left( \frac{1}{2} v_3^2 + (u_2 - v_2)^2 \right) u_3^2 + \frac{1}{2} v_3^4 \right) k u_3^2 v_3 e^{-\frac{(u_2 - v_2)^2}{u_3^2 + v_3^2}} \right. \right. \\
&\quad \left. \left. + \left( (u_4^2 (u_5 d_r + \frac{p_r}{3}) u_3^4 - 4 (d u_5 + \frac{p_i}{3}) u_4 u_3^2 - 4 u_5 d_r - \frac{4}{3} p_r \right) \sqrt{2} + \frac{4 u_1^2 (u_1^2 \sqrt{6} c_r + \frac{9}{4} q_r) u_3^2}{27} \right) \right. \\
&\quad \left. u_1 (u_3^2 + v_3^2)^{5/2} \right] \\
\dot{u}_5 &= \frac{3}{16} \left[ \frac{\sqrt{2}}{(u_3^2 + v_3^2)^{\frac{3}{2}} u_3^4 u_1} \left( -\frac{32 u_3^6 u_4 k v_1 v_3 (u_2 - v_2)}{3} e^{-\frac{(u_2 - v_2)^2}{u_3^2 + v_3^2}} + (d_i u_3^4 u_4^2 + (4 d_i u_5^2 + \frac{8}{3} p_i u_5) u_3^2 \right. \right. \\
&\quad \left. \left. + 4 d_i \right) (u_3^4 u_4^2 + 4) u_1 \sqrt{2} (u_3^2 + v_3^2)^{\frac{3}{2}} \right] \\
\dot{u}_6 &= \frac{3}{16} \left[ \frac{\sqrt{2}}{(u_3^2 + v_3^2)^{\frac{5}{2}} u_3^2 u_1} \left( \right. \right. \\
&\quad \left. \left. - \frac{32 v_1 k (u_5 (u_2 - v_2) u_3^4 + ((\frac{1}{2} + u_5 (u_2 - v_2)) v_3^2 + (u_2 - v_2)^2) u_3^2 + \frac{1}{2} v_3^4) u_3^2 v_3}{3} e^{-\frac{(u_2 - v_2)^2}{u_3^2 + v_3^2}} \right. \right. \\
&\quad \left. \left. + \left( (d_i u_3^6 u_4^3 u_5 + 2 u_5 u_4 (2 d_i u_5^2 + d_r u_4 + \frac{4}{3} p_i u_5) u_3^4 + (-4 d_i u_4 u_5 + \frac{8}{3} \gamma_i + \frac{8}{3} p_r u_5^2 - \frac{8}{3} p_i u_4 \right. \right. \right. \\
&\quad \left. \left. + \frac{16}{3} d_r u_5^3) u_3^2 - \frac{16}{3} p_r - 8 u_5 d_r \right) \sqrt{2} + \frac{32 u_1^2 u_3^2}{27} \left( u_1^2 \sqrt{6} c_r + \frac{45 q_r}{16} \right) \right] u_1 (u_3^2 + v_3^2)^{\frac{5}{2}} \right], \tag{A.1}
\end{aligned}$$

and:

$$\begin{aligned}
v_1 &= -\frac{2}{9} \left[ \frac{\sqrt{2}}{(u_3^2 + v_3^2)^{\frac{5}{2}} v_3^2} (9 v_3^2 u_1 (-\frac{3}{4} v_3^4 + (-u_3 + u_2 - v_2)(u_3 + u_2 - v_2)v_3^2 - \frac{1}{4} u_3^4) k u_3 e^{-\frac{(u_2 - v_2)^2}{u_3^2 + v_3^2}} \right. \\
&\quad + (u_3^2 + v_3^2)^{\frac{5}{2}} ((-\frac{9}{4} d_i v_5^3 + \frac{27 d_r v_4 v_5}{4} - \frac{9}{4} p_i v_5^2 + \frac{9}{4} p_r v_4 - \frac{9}{4} \gamma_r) v_3^2 - \frac{27 d_i v_5}{2} - \frac{9}{2} p_i) \sqrt{2} \\
&\quad \left. + v_1^2 v_3^2 (v_1^2 \sqrt{6} c_i + \frac{45 q_i}{16}) v_1 \right] \\
v_2 &= \frac{3}{16} \left[ \frac{\sqrt{2}}{(u_3^2 + v_3^2)^{\frac{3}{2}} v_3^2 v_1} \left( \frac{32 k v_3^4 u_3 u_1 (u_2 - v_2)}{3} e^{-\frac{(u_2 - v_2)^2}{u_3^2 + v_3^2}} + (u_3^2 + v_3^2)^{\frac{3}{2}} \sqrt{2} v_1 (d_i v_3^6 v_4^3 \right. \right. \\
&\quad \left. \left. + 2(2 d_i v_5^2 + d_r v_4 + \frac{4}{3} p_i v_5) v_4 v_3^4 + (4 d_i v_4 + 8(v_5 d_r + \frac{2}{3} p_r) v_5) v_3^2 + 8 d_r \right) \right] \\
v_3 &= \frac{1}{9} \left[ \frac{\sqrt{2}}{(u_3^2 + v_3^2)^{\frac{5}{2}} v_1 v_3} (36 v_3^2 u_1 k \right. \\
&\quad \left. (-\frac{1}{4} v_3^4 + v_3^2 (u_2 - v_2)^2 + \frac{1}{4} u_3^4) u_3 e^{-\frac{(u_2 - v_2)^2}{u_3^2 + v_3^2}} + (u_3^2 + v_3^2)^{\frac{5}{2}} \left( \frac{(27 d_i v_5 + 9 p_i) v_4^2 v_3^4}{4} \right. \right. \\
&\quad \left. \left. + 27(v_5 d_r + \frac{p_r}{3}) v_4 v_3^2 - 27 d_i v_5 - 9 p_i \right) \sqrt{2} + v_1^2 v_3^2 (v_1^2 \sqrt{6} c_i + \frac{9}{4} q_i) v_1 \right] \\
v_4 &= -\frac{4}{9} \left[ \frac{\sqrt{2}}{(u_3^2 + v_3^2)^{\frac{5}{2}} v_3^4 v_1} (-36 v_3^2 \left( \frac{1}{2} u_3^2 + (u_2 - v_2)^2 \right) v_3^2 + \frac{1}{2} u_3^4) u_1 k u_3 e^{-\frac{(u_2 - v_2)^2}{u_3^2 + v_3^2}} \right. \\
&\quad + (u_3^2 + v_3^2)^{\frac{5}{2}} \left( \frac{(27 v_5 d_r + 9 p_r) v_4^2 v_3^4}{4} - 27(d_i v_5 + \frac{p_i}{3}) v_4 v_3^2 - 27 v_5 d_r - 9 p_r \right) \sqrt{2} \\
&\quad \left. + v_1^2 v_3^2 (v_1^2 \sqrt{6} c_r + \frac{9}{4} q_r) v_1 \right] \\
v_5 &= 2 \left[ \frac{\sqrt{2}}{(u_3^2 + v_3^2)^{\frac{3}{2}} v_3^4 v_1} \left( \frac{3(u_3^2 + v_3^2)^{\frac{3}{2}} (d_i v_3^4 v_4^2 + (4 d_i v_5^2 + \frac{8}{3} p_i v_5) v_3^2 + 4 d_i) \sqrt{2} (v_3^4 v_4^2 + 4) v_1}{32} \right. \right. \\
&\quad \left. \left. + v_3^6 v_4 k u_3 u_1 (u_2 - v_2) e^{-\frac{(u_2 - v_2)^2}{u_3^2 + v_3^2}} \right) \right] \\
v_6 &= \frac{2}{9} \left[ \frac{\sqrt{2}}{(u_3^2 + v_3^2)^{\frac{5}{2}} v_3^2 v_1} (-9 v_3^2 (-v_5 (u_2 - v_2) v_3^4 + \left( \frac{1}{2} + (v_2 - u_2) v_5 \right) u_3^2 + (u_2 - v_2)^2) v_3^2 \right. \\
&\quad + \frac{1}{2} u_3^4) u_1 k u_3 e^{-\frac{(u_2 - v_2)^2}{u_3^2 + v_3^2}} + \left( \frac{27 d_i v_3^6 v_4^3 v_5}{32} + \frac{27 v_5 (2 d_i v_5^2 + d_r v_4 + 4/3 p_i v_5) v_4 v_3^4}{16} + \left( -\frac{27 d_i v_4 v_5}{8} + \frac{9}{4} \gamma_i \right. \right. \\
&\quad \left. \left. + \frac{9}{4} v_5^2 p_r - \frac{9}{4} p_i v_4 + \frac{9}{2} v_5^3 d_r \right) v_3^2 - \frac{9}{2} p_r - \frac{27 v_5 d_r}{4} \right) \sqrt{2} + v_1^2 v_3^2 (v_1^2 \sqrt{6} c_r + \frac{45 q_r}{16}) (u_3^2 + v_3^2)^{\frac{5}{2}} v_1 \right]. \tag{A.2}
\end{aligned}$$

## References

## References

- [1] I. S. Aranson, L. Kramer, The world of the complex ginzburg-landau equation, *Reviews of Modern Physics* 74 (1) (2002) 99.
- [2] Complex ginzburglandau equation, in: A. scott (ed.), *encyclopedia of nonlinear science*.
- [3] H. G. Winful, D. T. Walton, Passive mode locking through nonlinear coupling in a dual-core fiber laser, *Optics letters* 17 (23) (1992) 1688–1690.
- [4] F. T. Arecchi, S. Boccaletti, P. Ramazza, Pattern formation and competition in nonlinear optics, *Physics Reports* 318 (1-2) (1999) 1–83.
- [5] M. Ipsen, L. Kramer, P. G. Sørensen, Amplitude equations for description of chemical reaction–diffusion systems, *Physics Reports* 337 (1-2) (2000) 193–235.
- [6] M. Ferrmann, A. Galvanauskas, G. Sucha, D. Harter, Fiber-lasers for ultrafast optics, *Applied Physics B: Lasers and Optics* 65 (2) (1997) 259–275.
- [7] Y. He, B. A. Malomed, H. Wang, Fusion of necklace-ring patterns into vortex and fundamental solitons in dissipative media, *Optics express* 15 (26) (2007) 17502–17508.

- [8] B. Liu, X.-D. He, S.-J. Li, Phase controlling of collisions between solitons in the two-dimensional complex ginzburg-landau equation without viscosity, *Physical Review E* 84 (5) (2011) 056607.
- [9] S. Lai, H. Li, Y. Qui, X. Zhu, D. Mihalache, B. A. Malomed, Y. He, Generation of ring-shaped optical vortices in dissipative media by inhomogeneous effective diffusion, *Nonlinear Dynamics* 93 (4) (2018) 2159–2168.
- [10] A. Moubissi, K. Nakkeeran, P. T. Dinda, T. Kofane, Non-lagrangian collective variable approach for optical solitons in fibres, *Journal of Physics A: Mathematical and General* 34 (1) (2001) 129.
- [11] B. A. Malomed, Solitary pulses in linearly coupled ginzburg-landau equations, *Chaos: An Interdisciplinary Journal of Nonlinear Science* 17 (3) (2007) 037117.
- [12] B. A. Malomed, A variety of dynamical settings in dual-core nonlinear fibers, *Handbook of Optical Fibers* (2017) 1–54.
- [13] B. A. Malomed, H. G. Winful, Stable solitons in two-component active systems, *Physical Review E* 53 (5) (1996) 5365.
- [14] J. Atai, B. A. Malomed, Stability and interactions of solitons in two-component active systems, *Physical Review E* 54 (4) (1996) 4371.
- [15] H. Sakaguchi, Phase dynamics of the coupled complex ginzburg-landau equations, *Progress of Theoretical Physics* 93 (3) (1995) 491–502.
- [16] H. Sakaguchi, Traveling wave–standing wave transition in the coupled complex ginzburg–landau equations, *Physica Scripta* 1996 (T67) (1996) 148.
- [17] H. Sakaguchi, B. A. Malomed, Instabilities and splitting of pulses in coupled ginzburg–landau equations, *Physica D: Nonlinear Phenomena* 154 (3-4) (2001) 229–239.
- [18] J. Atai, B. A. Malomed, Exact stable pulses in asymmetric linearly coupled ginzburg-landau equations, *Physics Letters A* 246 (5) (1998) 412–422.
- [19] H. Sakaguchi, B. A. Malomed, Breathing and randomly walking pulses in a semilinear ginzburg–landau system, *Physica D: Nonlinear Phenomena* 147 (3-4) (2000) 273–282.
- [20] S. Jensen, The nonlinear coherent coupler, *IEEE Journal of Quantum Electronics* 18 (10) (1982) 1580–1583.
- [21] A. Govindaraji, A. Mahalingam, A. Uthayakumar, Femtosecond pulse switching in a fiber coupler with third order dispersion and self-steepening effects, *Optik-International Journal for Light and Electron Optics* 125 (15) (2014) 4135–4139.
- [22] A. Govindaraji, A. Mahalingam, A. Uthayakumar, Numerical investigation of dark soliton switching in asymmetric nonlinear fiber couplers, *Applied Physics B* 120 (2) (2015) 341–348.
- [23] A. Govindaraji, A. Mahalingam, A. Uthayakumar, Dark soliton switching in nonlinear fiber couplers with gain, *Optics & Laser Technology* 60 (2014) 18–21.
- [24] A. K. Sarma, Dark soliton switching in an nldc in the presence of higher-order perturbative effects, *Optics & Laser Technology* 41 (3) (2009) 247–250.
- [25] A. K. Sarma, Vector soliton switching in a fiber nonlinear directional coupler, *Optics communications* 284 (1) (2011) 186–190.
- [26] A. Govindarajan, B. A. Malomed, M. Lakshmanan, Nonlinear anti-directional couplers with gain and loss, *Optics Letters* 44 (19) (2019) 4650–4653.
- [27] A. Govindarajan, A. K. Sarma, M. Lakshmanan, Tailoring pt-symmetric soliton switch, *Optics letters* 44 (3) (2019) 663–666.
- [28] A. Govindaraji, A. Mahalingam, A. Uthayakumar, Interaction dynamics of bright solitons in linearly coupled asymmetric systems, *Optical and Quantum Electronics* 48 (12) (2016) 563.
- [29] D. Correia, W. de Fraga, G. Guimarães, et al., Obtaining optical logic gates–or, xor, and and logic functions using asymmetric mach-zehnder interferometer based on photonic crystal fiber, *Optics & Laser Technology* 97 (2017) 370–378.
- [30] R. Ganapathy, B. A. Malomed, K. Porsezian, Modulational instability and generation of pulse trains in asymmetric dual-core nonlinear optical fibers, *Physics Letters A* 354 (5-6) (2006) 366–372.
- [31] A. Govindarajan, B. Malomed, A. Mahalingam, A. Uthayakumar, Modulational instability in linearly coupled asymmetric dual-core fibers, *Applied Sciences* 7 (7) (2017) 645.
- [32] J. H. Li, K. S. Chiang, K. W. Chow, Modulation instabilities in two-core optical fibers, *JOSA B* 28 (7) (2011) 1693–1701.
- [33] J. Li, K. S. Chiang, B. Malomed, K. Chow, Modulation instabilities in birefringent two-core optical fibres, *Journal of Physics B: Atomic, Molecular and Optical Physics* 45 (16) (2012) 165404.
- [34] Y. Kominis, T. Bountis, S. Flach, Stability through asymmetry: Modulationally stable nonlinear supermodes of asymmetric non-hermitian optical couplers, *Physical Review A* 95 (6) (2017) 063832.
- [35] Y. Zhiyenbayev, Y. Kominis, C. Valagiannopoulos, V. Kovanis, A. Bountis, Enhanced stability, bistability, and exceptional points in saturable active photonic couplers, *Physical Review A* 100 (4) (2019) 043834.
- [36] B. A. Malomed, G. Peng, P. Chu, Nonlinear-optical amplifier based on a dual-core fiber, *Optics letters* 21 (5) (1996) 330–332.
- [37] P. Chu, B. A. Malomed, G. Peng, Pulse propagation through a nonlinear optical amplifier, *Optics communications* 140 (4-6) (1997) 289–295.
- [38] D. T. Walton, H. G. Winful, Passive mode locking with an active nonlinear directional coupler: positive group-velocity dispersion, *Optics letters* 18 (9) (1993) 720–722.
- [39] J. Kaňka, Numerical simulation of subpicosecond soliton formation in a nonlinear coupler laser, *Optics letters* 19 (22) (1994) 1873–1875.
- [40] Y. Oh, S. Doty, J. Haus, R. Fork, Robust operation of a dual-core fiber ring laser, *JOSA B* 12 (12) (1995) 2502–2507.
- [41] A. Sigler, B. A. Malomed, Solitary pulses in linearly coupled cubic–quintic ginzburg–landau equations, *Physica D: Nonlinear Phenomena* 212 (3-4) (2005) 305–316.
- [42] K. Porsezian, R. Murali, B. A. Malomed, R. Ganapathy, Modulational instability in linearly coupled complex cubic–quintic ginzburg–landau equations, *Chaos, Solitons & Fractals* 40 (4) (2009) 1907–1913.
- [43] J. Alcaraz-Pelegriña, P. Rodríguez-García, Modulational instability in two cubic–quintic ginzburg–landau equations coupled with a cross phase modulation term, *Physics Letters A* 374 (13-14) (2010) 1591–1599.
- [44] A. Berntson, B. A. Malomed, Dispersion management with filtering, *Optics letters* 24 (8) (1999) 507–509.
- [45] B. A. Malomed, Soliton management in periodic systems, Springer Science & Business Media, 2006.
- [46] S. T. B. Wong, Dispersion-managed solutions in the path-average normal dispersion regime, Ph.D. thesis, Massachusetts Institute of Technology (2001).
- [47] S. Fewo, J. Atangana, A. Kenfack-Jiotsa, T. Kofane, Dispersion-managed solitons in the cubic complex ginzburg–landau equation as pertur-



- bations of nonlinear schrödinger equation, *Optics Communications* 252 (1-3) (2005) 138–149.
- [48] S. Fewo, T. Kofane, A collective variable approach for optical solitons in the cubic–quintic complex ginzburg–landau equation with third-order dispersion, *Optics Communications* 281 (10) (2008) 2893–2906.
- [49] A. Biswas, et al., Femtosecond pulse propagation in optical fibers under higher order effects: A collective variable approach, *International Journal of Theoretical Physics* 47 (6) (2008) 1699–1708.
- [50] H. Sakaguchi, D. V. Skryabin, B. A. Malomed, Stationary and oscillatory bound states of dissipative solitons created by third-order dispersion, *Optics letters* 43 (11) (2018) 2688–2691.
- [51] R. B. Djob, A. Kenfack-Jiotsa, T. C. Kofané, Study of the effect of the coupling in a dispersion-managed dual core optical fiber using the collective variables approach, *Journal of Applied Nonlinear Dynamics* 4 (2) (2015) 101–116.
- [52] P. D. Green, D. M. Milovic, D. A. Lott, A. Biswas, Dynamics of gaussian optical solitons by collective variables method, *Applied Mathematics and Information Sciences* 2 (3) (2008) 259–273.
- [53] K. Tamilselvan, T. Kanna, A. Govindarajan, Cubic-quintic nonlinear helmholtz equation: Modulational instability, chirped elliptic and solitary waves, *Chaos: An Interdisciplinary Journal of Nonlinear Science* 29 (6) (2019) 063121.
- [54] M. Veljkovic, Y. Xu, D. Milovic, M. Mahmood, A. Biswas, M. R. Belic, Super-gaussian solitons in optical metamaterials using collective variables, *Journal of Computational and Theoretical Nanoscience* 12 (12) (2015) 5119–5124.
- [55] M. Veljković, D. Milovic, M. Belić, Q. Zhou, S. P. Moshokoa, A. Biswas, Super-sech soliton dynamics in optical metamaterials using collective variables, *Facta Universitatis, Series: Electronics and Energetics* 30 (1) (2016) 39–48.
- [56] M. Asma, W. Othman, B. Wong, A. Biswas, Chirped optical gaussian perturbation with quadratic–cubic nonlinearity by collective variables, *Optical and Quantum Electronics* 51 (6) (2019) 200.